(Received 7 October 2024, Accepted 30 December 2024, Scheduled 24 January 2025)

A Compact Wideband Two-Port mm-Wave Antenna for 5G Application

Rajeshwari Malekar[1,2], Saffrine Kingsly[2,*], Sangeetha Subbaraj[3], and Hema Raut[2,4]

[1]*Electronics and Telecommunication Department*
Marathwada Mitra Mandal's College of Engineering, Pune, Maharashtra, India
[2]*Electronics and Telecommunication Department*
Symbiosis Institute of Technology, Symbiosis International (Deemed University), Pune, India
[3]*Department of Electronics and Communication Engineering*
College of Engineering, Guindy, Anna University, Chennai, India
[4]*Electronics and Computer Science Department*
South Indian Education Society-Graduate School of Technology, Nerul, India

ABSTRACT: This study presents the design of a MIMO (multiple inputs, multiple outputs) antenna for the 5G application. This is an inexpensive, low-profile antenna with a dimension of $9 \times 18 \times 1\,\text{mm}^3$. The highest gain of the antenna in the operating frequency range is 7.79 dBi. This antenna structure provides a minimum isolation of less than -20 dB for the working bandwidth. The antenna's operational bandwidth covers the 26 GHz band mm-wave (millimeter-wave) spectrum, from 26.86 to 31.11 GHz. Its salient features make it appropriate for 5G applications.

1. INTRODUCTION

In the realm of IoT (Internet of Things) and smart home living, there has been a recent surge in demand for maximum throughput and high data rates. It was aided by the development of wireless technology, especially with the upcoming 5G mobile communication. It presents more challenges as well as opportunities for any antenna designer. 5G technology requires an antenna with low latency, stable radiation pattern, and low path loss.

Mobility, frequency ranges, forward error correction, data rate, latency, connection dependability, access technology, and spectral efficiency are the features of 5G technologies [1–3]. ITU-R divides the frequency spectrum of 5G into two groups: Frequency ranges 1 (FR1) and 2 (FR2) of the below 6 GHz and above 6 GHz bands [1]. FR1 Frequencies: 450 MHz to 7.125 GHz and FR2 Frequencies: 24.25 GHz to 52.6 GHz. Wideband and multiband antenna designs have been the subject of extensive research. However, the most talked-about technology currently relates to millimeter waves, specifically the 24–100 GHz spectrum. The increased need for low latency, high data throughput, and limited bandwidth in the microwave frequency band led to the utilization of this band by 5G systems. Thus, mm-wave antenna design has gained significance in recent years.

5G antennas can be categorized based on how many input and output ports they have. Antennas are divided into three categories: metal rim antennas, multiple input multiple output (MIMO) antennas, and single input single output (SISO) antennas [1, 4]. They come under the group of multiband and wideband antennas. Many researchers have been using SISO antennas for 5G applications due to the ease of deployment and design. The propagation loss occurs when frequencies above 6 GHz are used, which requires the usage of several antennas, and they are more expensive and require a more intricate design [5]. The main limitation of the SISO system is data rate, which MIMO systems can overcome [6].

MIMO uses more broadcast and receive antennas to boost the link's capacity. This allows multiple channels to be delivered and received via the radio link simultaneously. The capacity of MIMO antennas increases transmission range without boosting signal intensity which is one of its key features. It is advised to use several antennas since they simplify the system beyond array antenna systems. MIMO antennas are utilized in 5G communication to obtain the best throughput, maximum efficiency, highest data rate, and lowest latency.

One of the main goals of the 5G antenna is to have a small size. On the other hand, mutual coupling is on the higher end when the antennas are closer together. The mutual coupling between the two antenna elements is enhanced by space radiation and the strong current flow from the exciting port to the non-excited port. Reducing mutual coupling among many antennas while maintaining antenna compactness is the main problem in 5G antenna design. To lessen the mutual coupling among numerous MIMO antennas, various decoupling techniques have been employed.

In this work, Ansys HFSS software is used to simulate the single patch and MIMO antenna. The structure of the paper is arranged as follows. Section 2 presents the geometry of a single patch antenna and MIMO antenna. It also provides the

* Corresponding author: Saffrine Kingsly (kingsly.saffrine@gmail.com).

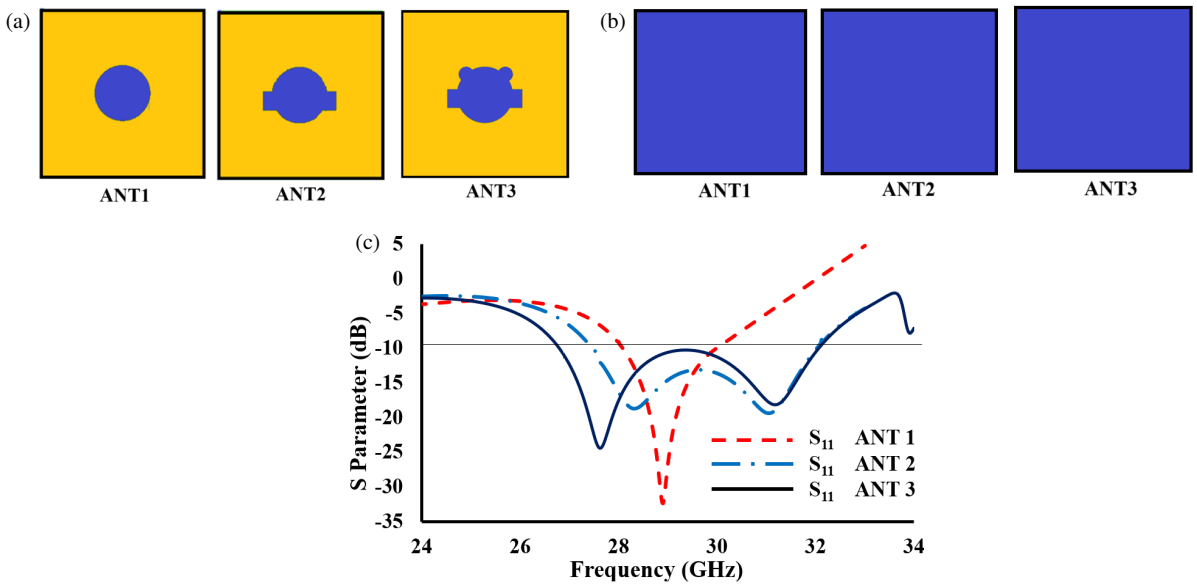

FIGURE 1. (a) Evolution of the 5G antenna (Front view). (b) Bottom view of the 5G antenna. (c) Reflection coefficient during each stage of evolution.

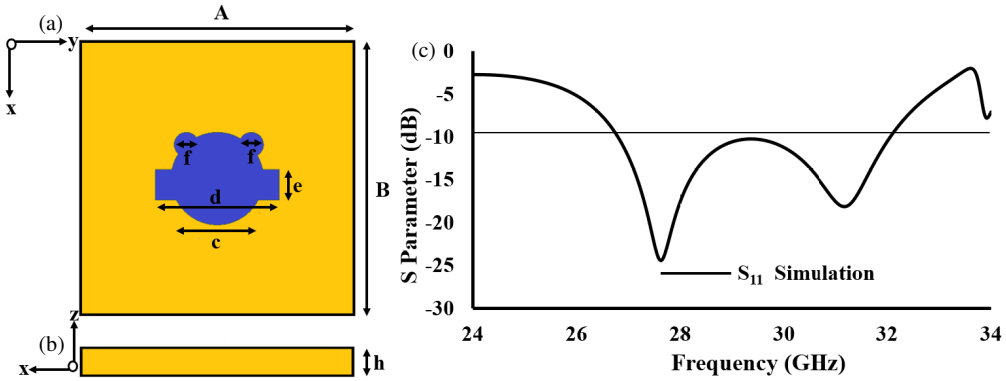

FIGURE 2. Single patch 5G antenna schematic diagram. (a) Top view: $A = 9\,\text{mm}$, $B = 9\,\text{mm}$, $c = 1.5\,\text{mm}$, $d = 4\,\text{mm}$, $e = 1\,\text{mm}$, $f = 0.4\,\text{mm}$. (b) Side view: $h = 0.8\,\text{mm}$. (c) Reflection coefficient (S_{11}).

simulated return loss and gain results of the antenna. Section 3 presents the antenna fabricated prototype and measured results for a single patch and MIMO antennas. Section 4 concludes the work.

2. ANTENNA DESIGN

The proposed antenna is designed on a Roger RT duroid 5880 substrate with dielectric constant $(\epsilon_r) = 2.2$ and $\tan\delta = 0.0009$. The method of coaxial feeding is applied to the proposed structure.

2.1. A Single Patch Antenna Design

Figure 1(a) depicts the evolution of the intended mm-wave single-patch antenna, and Figure 1(b) shows the evolution of the ground plane. Figure 1(c) depicts the S_{11} of each evolutionary step of the antenna design. Ant 1 is a circular patch antenna that resonates around 29 GHz in the first stage of antenna design. The circular patch is determined using Equations (1) and (2) as in [7]. To resonate at a lower frequency and prolong the bandwidth, a rectangular structure is added to the circular patch. Now, the antenna resonates from 27.46 GHz. In the last stage, the circular construction is installed on both the right and left sides of the antenna structure, as represented by Ant 3.

$$a = \frac{F}{\sqrt{1 + \frac{2h}{\Pi\epsilon_r F}\left[\text{In}\left(\frac{\Pi F}{2h}\right) + 1.7726\right]}} \tag{1}$$

$$F = \frac{8.791 \times 10^9}{f_r\sqrt{\epsilon_r}} \tag{2}$$

The substrate dimension of the single patch antenna is $9 \times 9\,\text{mm}^2$. The geometry of the proposed linearly polarized mm-wave single patch antenna is depicted in Figure 2(a), which also contains the optimal value of the designed antenna. Figure 2(b) presents the side view of the antenna. Figure 2(c) depicts the scattering parameter result. Based on the simu-

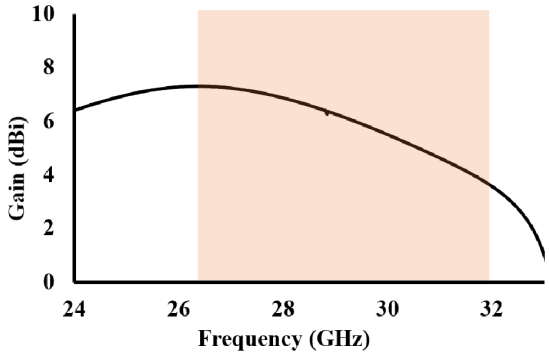

FIGURE 3. Gain of the designed mm-wave antenna.

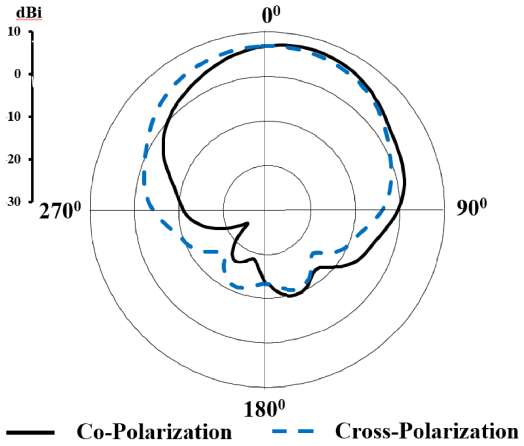

FIGURE 4. Single patch antenna structure E-plane co-polarization and cross polarization at 28 GHz.

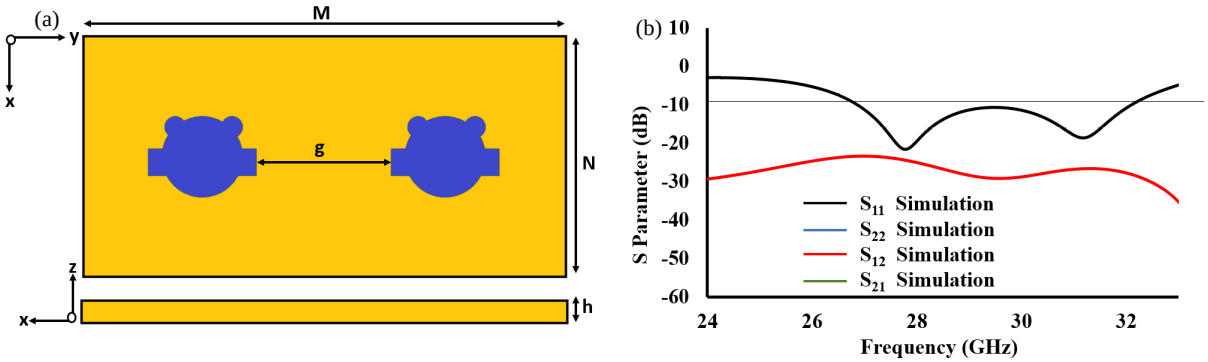

FIGURE 5. The two-port MIMO antenna's geometry. (a) MIMO structure $M = 18$ mm, $N = 9$ mm, $g = 5$ mm, $h = 0.8$ mm. (b) S-parameter (S_{11}, S_{22}, S_{12}, and S_{21}).

lated outcome shown in Figure 2(c), the antenna bandwidth is 5.36 GHz (26.80 GHz to 32.06 GHz).

The overall gain is shown in Figure 3, which exceeds 4 dBi, with a maximum gain up to 7.21 dBi being attained from 26.8 GHz to 27.08 GHz of frequency band. The maximum gain of up to 7.21 dBi being attained from 26.8 GHz to 27.08 GHz of frequency band. Cross-polarization and co-polarization in the E-plane for a single patch antenna are shown in Figure 4. The E-plane co-polarization and cross-polarization show that at the simulated frequency, resonances or depolarization effects cause similar energy distribution in the two polarizations.

2.2. MIMO Antenna Design

Due to the increasing demand for IoT and smart devices, 5G technology is predicted to deliver a considerably faster data rate, link stability, and better device capacity. A MIMO antenna is the primary component needed for a 5G antenna. Figure 5(a) illustrates the construction of a two-port MIMO structure. The substrate is shared by two antennas using a $9 \times 18\,\text{mm}^2$ substrate.

One of the main features to be focused on during the 5G antenna design is size reduction. However, the reduction in the distance between the antennas results in an increase in mutual coupling. When two antennas are placed close to each other, mutual coupling can alter the resonance frequencies and, consequently, the antennas bandwidth [8, 9]. Due to size constraints, compact MIMO antennas, that is, structures with inter-element spacing of less than half a wavelength [10], must be used in applications, such as mobile terminals and implantable devices [11]. In the proposed system distance between the antennas is optimized such that the mutual coupling remains less than -20 dB. The distance between the two antenna geometries, i.e., spacing between the two antennas, is less than $\lambda/4$ as compared to wavelength.

Since in proposed system the two antennas geometries are kept constant, the bandwidth of each antenna remains constant. The acquired bandwidth stays constant with the bandwidth obtained for a single patch antenna operating in the 26.86 GHz to 32.11 GHz frequency range. It is required that the mutual coupling should be less than -20 dB. Less than -20 dB of isolation is attained over the full bandwidth in the suggested configuration. The mutual coupling and reflection coefficient between the antennas are displayed in Figure 5(b). The current distribution of a two-port antenna structure at 29 GHz is presented in Figure 6. In Figure 7, the MIMO antenna gain is presented. The maximum gain achieved in the operating frequency range is up to 7.79 dBi [from 27.48 GHz to 27.9 GHz]. Comparative gains of single patch and MIMO antennas are presented in Figure 7. It shows that MIMO antenna gain is slightly greater than

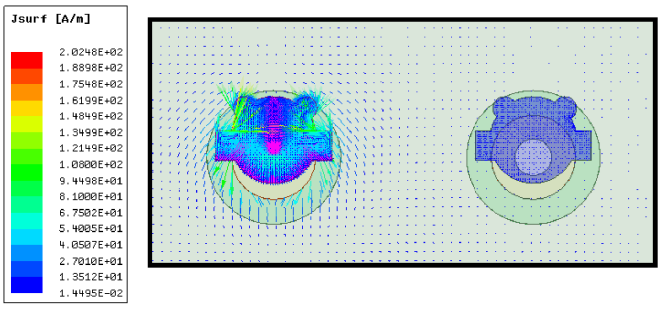

FIGURE 6. The current distribution of two elements antenna geometry at 29 GHz.

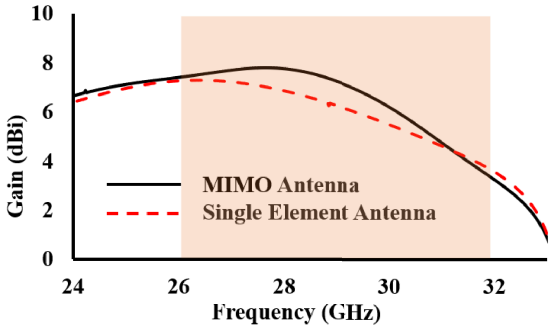

FIGURE 7. MIMO and single patch gain comparison of the mm-wave antenna.

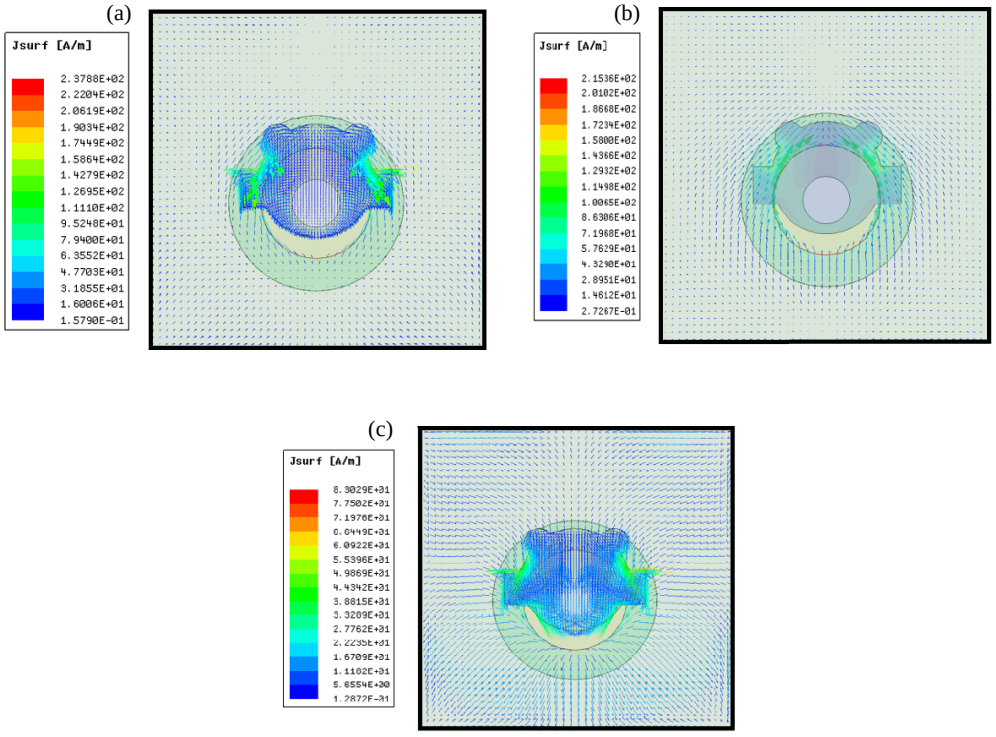

FIGURE 8. The current distributions of the antenna at different frequencies. (a) 26.87 GHz, (b) 29 GHz, (c) 32.13 GHz.

single patch antenna design. The surface current distributions at different frequencies are plotted in Figure 8.

3. RESULT AND DISCUSSION

The outcomes of the experiments and simulations are examined in this section. Ansys HFSS is used for simulation and analysis.

3.1. Single Patch Antenna

Measured and simulated S_{11} of the 5G MIMO structure using the fabricated prototype are shown in Figure 9. The antenna's configuration exhibits acceptable impedance matching, demonstrated by this figure, which is less than -10 dB. According to the measured data, the antenna's bandwidth is 5.62 GHz (26.6 GHz to 32.22 GHz). In simulations, the peak S_{11} is -24.48 dB, while in measurements, it is -25.83 dB.

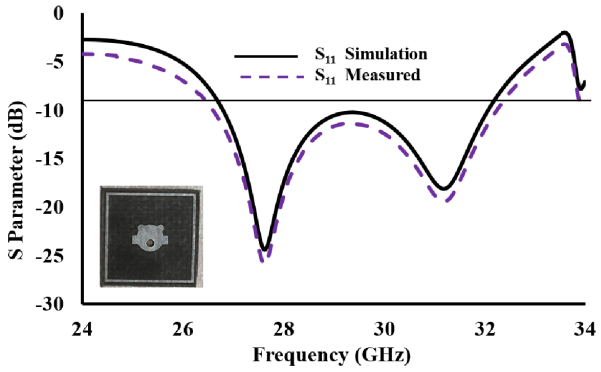

FIGURE 9. Simulated and measured S-parameter results for single patch antenna geometry with fabricated prototype.

3.2. Results for MIMO Antenna Structure

According to the measured data, the antenna's bandwidth is 5.62 GHz (26.6 GHz to 32.22 GHz). In simulations, the peak

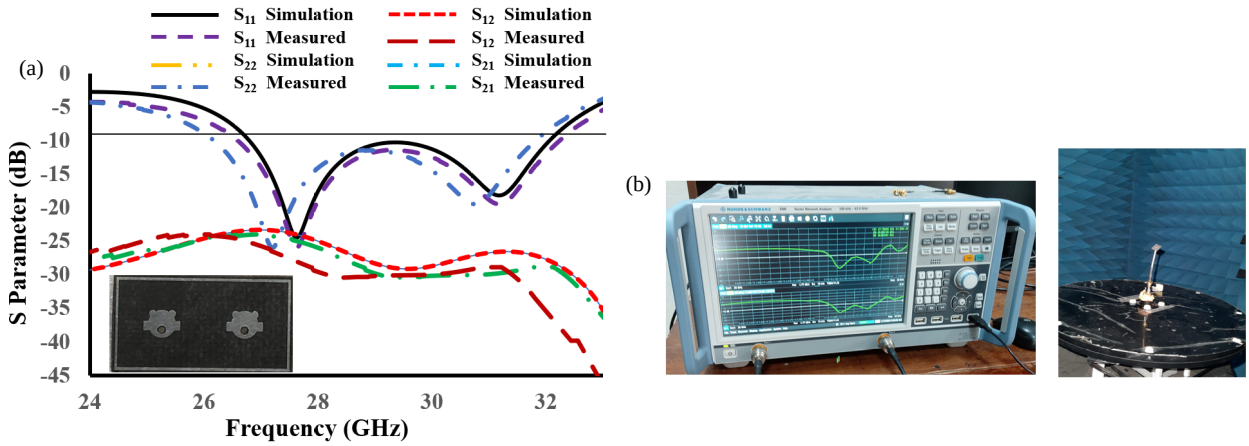

FIGURE 10. (a) Simulated and measured S-parameter results for MIMO antenna geometry with fabricated prototype. (b) Measurement setup.

TABLE 1. Comparison between the performances of the proposed MIMO antennas and the existing state of art.

Ref.	Size (mm^2)	Substrate	Peak Gain (dBi)	Freq. (GHz)	No. of Ports	Isolation	ECC	Diversity Gain (dB)	Efficiency (%)	Bandwidth (GHz)
[12]	$1.89\lambda \times 2.62\lambda$	Rogers RO4003C	11.9	28.45	2	-37	< 0.00025	10	91	3.8(26.9–30.7)
[13]	$1.87\lambda \times 1.87\lambda$	Rogers 5880	9	28	2	24	0.013	9.9	-	0.85(27.5–28.35)
[14]	$14.65\lambda \times 6.53\lambda$	Rogers 5880	8.2 8.7	28 38	8	> 25	< 0.35	9.9 9.95	98 97.6	1.2(27.15–28.35) 0.81(37.59–38.4)
[15]	$2.75\lambda \times 3.38\lambda$	Rogers 6010	6.4	26	2	30	0.002	-	-	1.9(25.2–27.1)
[16]	$3.03\lambda \times 3.03\lambda$	Roger 6002	6.6–9.1 9.3–9.9	26 35	4	22 17	< 0.001	> 9.97	96	3(24.50–27.50) 4(33–37)
[17]	$2.8\lambda \times 1.4\lambda$	Rogers 4003	5.42	28	2	-35.8	< 0.005	> 9.99	84	6.4(26.5–32.9)
[18]	$2.42\lambda \times 1.30\lambda$	AD250	7.4 6.2	28 38	2	34.6 47	0.2×10^{-4}	> 9.99	-	1.7(27.1–28.8) 3.7(35.2–38.9)
[19]	$1.24\lambda \times 4.89\lambda$	Rogers RT6002	10	38	4	> 30	2.7×10^{-8}	> 9.99	90	2.78(36.5–39.28)
[20]	$5.6\lambda \times 5.6\lambda$	Rogers RT5880	8.14 8.04	28 38	4	30	0.0035	9.982	99	3.05(27.35–30.40) 2.41(36.98–39.398)
Proposed work	$0.87\lambda \times 1.74\lambda$	Rogers 5880	7.79	29	2	-34.99	0.00044	10	99.83	5.36(26.80–32.06)

S_{11} is -24.48 dB, while in measurements it is -25.83 dB. The design of small antennas is one of the main issues in antenna design. Reducing the distance between the antenna structures results in a decrease in isolation. Antenna structural isolation must be less than -20 dB. The lowest isolation of -28 dB is attained in the MIMO antenna configuration. The isolation between the MIMO antenna structures is displayed in Figure 10. The measurement result indicates a maximum isolation of -34.99 dB between antennas 1 and 2.

The E-plane and H-plane radiation patterns are shown in Figures 11(a), (b), and (c). They present the co-polarization and cross-polarization for the MIMO structure. Simulated and measured gains for single patch and MIMO are presented in Figure 12. The comparison of the proposed microstrip antenna design with earlier studies is shown in Table 1. Comparison demonstrates that the MIMO antenna structures are smaller than the earlier antennas described in Table 1. The total efficiency of the suggested antenna is displayed in Figure 13. The suggested mm-wave MIMO antenna is shown to attain

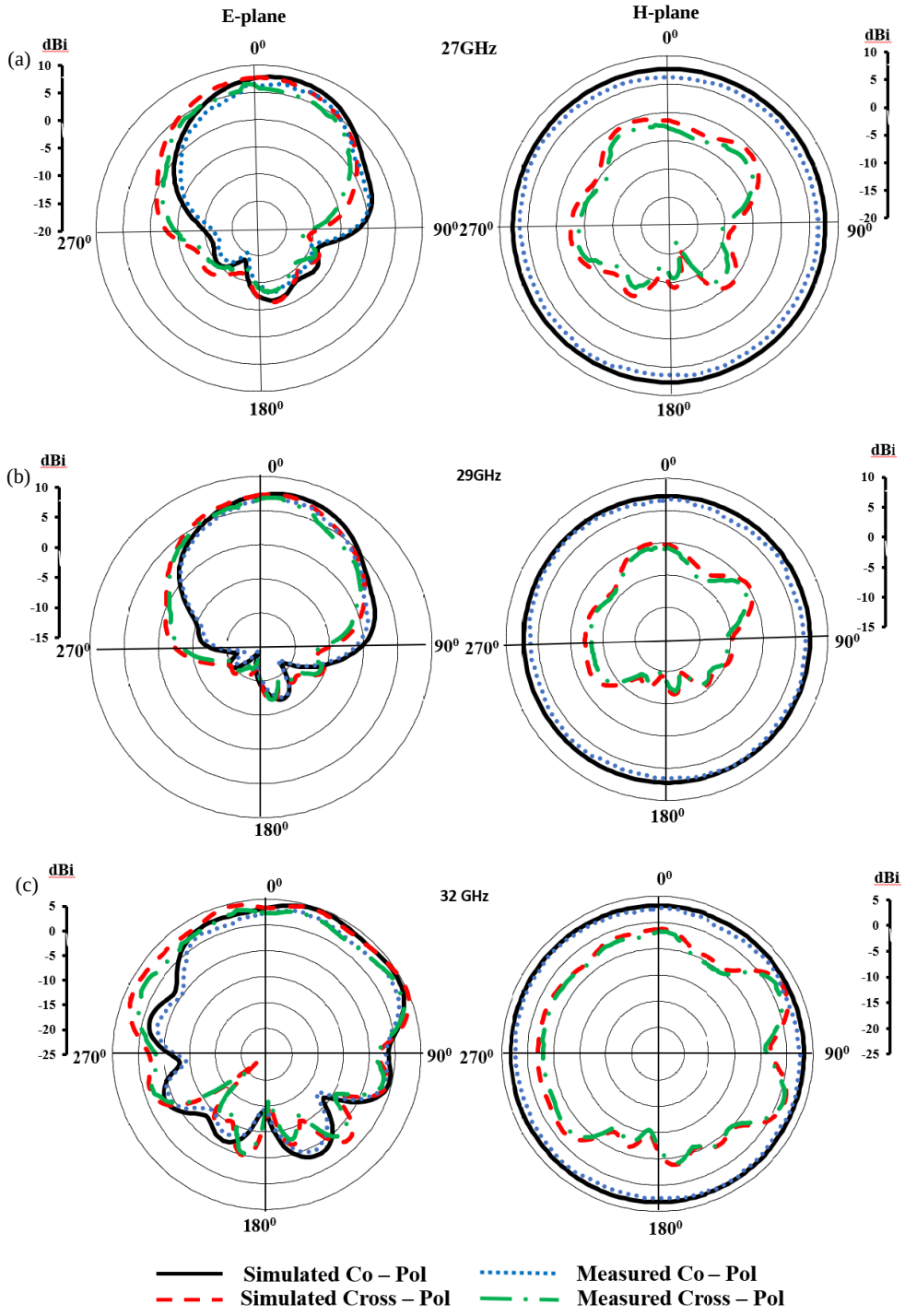

FIGURE 11. Measured and simulated millimeter-wave MIMO antenna radiation patterns at various frequencies. (a) 27 GHz, (b) 29 GHz, (c) 32 GHz.

an efficiency greater than 90% in the targeted band. Several measures, including ECC (Envelope Correlation Coefficient), MEG (Mean Effective Gain), and DG (Diversity Gain), are used to validate the performance of the MIMO antenna. In addition to providing a high diversity gain, multiple antenna structures should demonstrate channel independence by having a low ECC value. The ECC and DG of the 2×2 mm-wave MIMO antenna are 0.00044 and 10 dB respectively as shown in Figure 14. The DG's value can be obtained using the formula provided in (3).

$$\mathrm{DG} = 10\sqrt{1 - \mathrm{ECC}^2} \tag{3}$$

$$\mathrm{ECC} = \frac{\sum_{l=1}^{\infty}\sum_{m=-1}^{l}\sum_{s=1}^{2} q_{sml}^{1}(q_{sml}^{2})^{*}}{\sqrt{\left(\sum_{l=1}^{\infty}\sum_{m=-1}^{l}\sum_{s=1}^{2} q_{sml}^{1}(q_{sml}^{1})^{*}\right)\left(\sum_{l=1}^{\infty}\sum_{m=-1}^{l}\sum_{s=1}^{2} q_{sml}^{2}(q_{sml}^{2})^{*}\right)}} \tag{4}$$

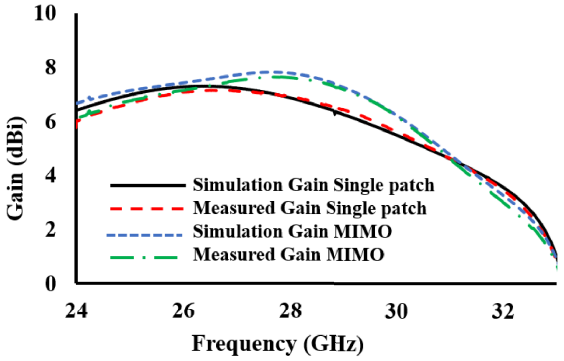

FIGURE 12. Measured and simulated gains.

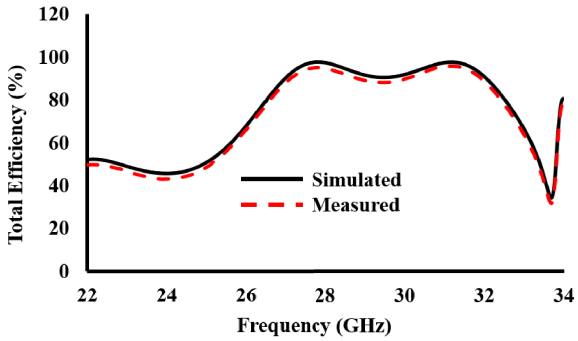

FIGURE 13. Total efficiency plot over the frequency band.

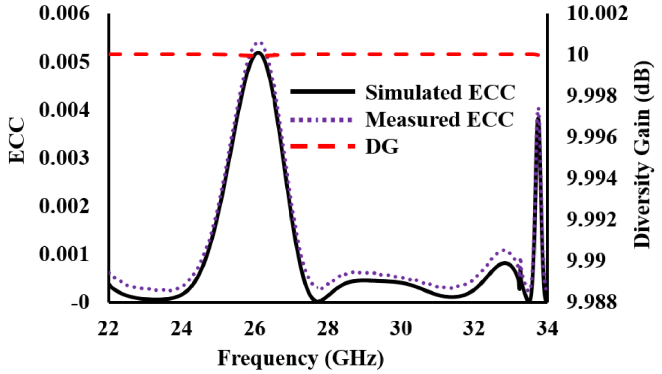

FIGURE 14. Simulated ECC and DG of proposed MIMO antenna.

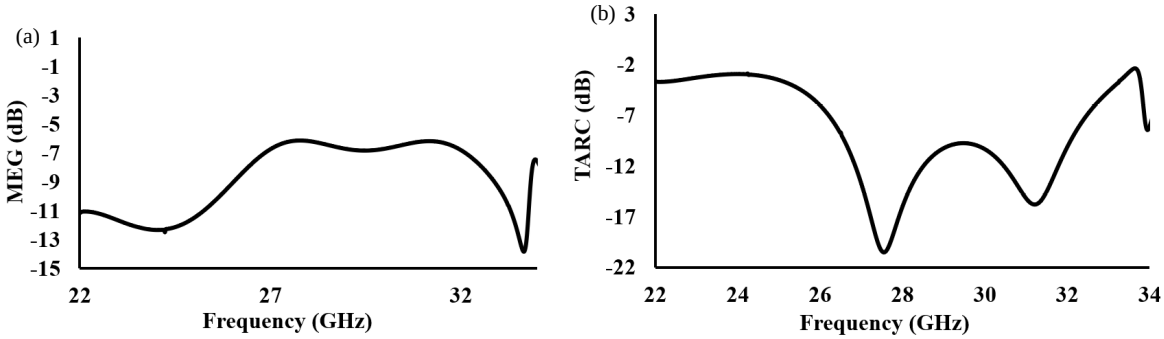

FIGURE 15. MEG and TARC of proposed MIMO antenna.

ECC can be calculated using the Equation (4) as in [21], where the complex coefficient of the spherical harmonic is denoted by qsml. Order m characterizes the field's azimuthal fluctuation, and both degree l and order m characterize the field's elevation changes. $(\cdot)^*$ denotes the complex conjugate, and the index $s = (1, 2)$ is associated with the elements of transversal electric and transversal magnetic waves.

TARC (Total Active Reflection Coefficient) takes mutual coupling and random signal combinations between ports into account. The simulated values of MEG and TARC are shown in Figure 15. Table 2 lists the values of diversity parameters such as ECC, MEG, and DG for various frequencies within the MIMO structure's bandwidth. The values of radiation efficiency and realised gain are also provided. These findings demonstrate the utility of the suggested antenna for MIMO operation.

3.3. Salient Features of the MIMO Antenna

1. In comparison to the antenna published in the literature [12–15, 17–20], the 5G antenna provided in this paper is compact.
2. Compared to [12–16, 18–20], this antenna has a broader bandwidth of 5.36 GHz, a low profile, and uncomplicated construction.
3. The small design, low cost, excellent radiation efficiency, and high diversity gains of the MIMO antenna set it apart from other relevant efforts that have been published in the literature.

TABLE 2. Diversity parameter, effective radiation, and realised gain.

Frequecy (GHz)	ECC	MEG1	MEG2	Diversity Gain (dB)	Radiation Efficiency (%)	Realised Gain (dB)
27	0.00163	−6.73	−6.74	9.99	99.23	7.34
28	0.00011	−6.15	−6.14	10	99.83	7.69
29	0.00044	−6.70	−6.70	10	99.83	6.90
30	0.00039	−6.68	−6.68	10	99.99	5.87
31	0.00014	−6.18	−6.18	10	99.99	4.67

4. The MIMO antenna provides low ECC, high diversity gains, compact design, and low cost.
5. The maximum frequency range of the n257 band (26.5 to 29.5 GHz) is covered in this study; the proposed structure spans from 26.8 to 32.06 GHz, which also includes the n261 band (27.5 to 28.35 GHz).

4. CONCLUSION

This low-profile and inexpensive millimeter-wave antenna is suitable for 5G applications. The MIMO antenna is 9 mm × 18 mm × 0.8 mm. The greatest impedance bandwidth offered by a single patch antenna and a MIMO antenna, according to simulated data, is 5.36 GHz (26.80 GHz to 32.06 GHz). Antenna gain is up to 7.79 dBi at maximum. The minimal isolation between antennas, according to the simulated findings, is less than −20 dB. The suggested antenna's ECC value is 0.00044. The received radiation efficiency is 99.83%. The suggested work has a diversity gain of 10. This antenna design has many qualities that make it beneficial for 5G applications.

REFERENCES

[1] Kumar, S., A. S. Dixit, R. R. Malekar, H. D. Raut, and L. K. Shevada, "Fifth generation antennas: A comprehensive review of design and performance enhancement techniques," *IEEE Access*, Vol. 8, 163 568–163 593, 2020.

[2] Huang, H.-C., "Overview of antenna designs and considerations in 5G cellular phones," in *2018 International Workshop on Antenna Technology (iWAT)*, 1–4, Nanjing, China, Mar. 2018.

[3] Hong, W., Z. H. Jiang, C. Yu, J. Zhou, P. Chen, Z. Yu, H. Zhang, B. Yang, X. Pang, M. Jiang, *et al.*, "Multibeam antenna technologies for 5G wireless communications," *IEEE Transactions on Antennas and Propagation*, Vol. 65, No. 12, 6231–6249, Dec. 2017.

[4] Khan, R., A. A. Al-Hadi, P. J. Soh, M. R. Kamarudin, M. T. Ali, *et al.*, "User influence on mobile terminal antennas: A review of challenges and potential solution for 5G antennas," *IEEE Access*, Vol. 6, 77 695–77 715, 2018.

[5] Liu, H., W. Yang, A. Zhang, S. Zhu, Z. Wang, and T. Huang, "A miniaturized gain-enhanced antipodal Vivaldi antenna and its array for 5G communication applications," *IEEE Access*, Vol. 6, 76 282–76 288, 2018.

[6] Nadeem, I. and D.-Y. Choi, "Study on mutual coupling reduction technique for MIMO antennas," *IEEE Access*, Vol. 7, 563–586, 2018.

[7] Balanis, C. A., "Microstrip antennas," in *Antenna Theory: Analysis and Design*, 843–848, 3rd Edition, John Wiley & Sons, Inc., Hoboken, New Jersey, USA, 2005.

[8] Zhang, Y., K. Hirasawa, and K. Fujimoto, "Signal bandwidth consideration of mutual coupling effects on adaptive array performance," *IEEE Transactions on Antennas and Propagation*, Vol. 35, No. 3, 337–339, Mar. 1987.

[9] Singh, H., H. L. Sneha, and R. M. Jha, "Mutual coupling in phased arrays: A review," *International Journal of Antennas and Propagation*, Vol. 2013, No. 1, 348123, 2013.

[10] Abdullah, M. and S. Koziel, "A novel versatile decoupling structure and expedited inverse-model-based re-design procedure for compact single- and dual-band MIMO antennas," *IEEE Access*, Vol. 9, 37 656–37 667, 2021.

[11] Bazaka, K. and M. V. Jacob, "Implantable devices: Issues and challenges," *Electronics*, Vol. 2, No. 1, 1–34, Dec. 2012.

[12] Ullah, U., M. Al-Hasan, S. Koziel, and I. B. Mabrouk, "Series-slot-fed circularly polarized multiple-input–multiple-output antenna array enabling circular polarization diversity for 5G 28 GHz indoor applications," *IEEE Transactions on Antennas and Propagation*, Vol. 69, No. 9, 5607–5616, Sep. 2021.

[13] Zhang, Y., J.-Y. Deng, M.-J. Li, D. Sun, and L.-X. Guo, "A MIMO dielectric resonator antenna with improved isolation for 5G mm-Wave applications," *IEEE Antennas and Wireless Propagation Letters*, Vol. 18, No. 4, 747–751, 2019.

[14] Islam, S., M. Zada, and H. Yoo, "Low-pass filter based integrated 5G smartphone antenna for sub-6-GHz and mm-Wave bands," *IEEE Transactions on Antennas and Propagation*, Vol. 69, No. 9, 5424–5436, Sep. 2021.

[15] Pan, Y. M., X. Qin, Y. X. Sun, and S. Y. Zheng, "A simple decoupling method for 5G millimeter-wave MIMO dielectric resonator antennas," *IEEE Transactions on Antennas and Propagation*, Vol. 67, No. 4, 2224–2234, Apr. 2019.

[16] Girjashankar, P. R. and T. Upadhyaya, "Substrate integrated waveguide fed dual band quad-elements rectangular dielectric resonator MIMO antenna for millimeter wave 5G wireless communication systems," *AEU — International Journal of Electronics and Communications*, Vol. 137, 153821, 2021.

[17] Hussain, N., W. A. Awan, W. Ali, S. I. Naqvi, A. Zaidi, and T. T. Le, "Compact wideband patch antenna and its MIMO configuration for 28 GHz applications," *AEU — International Journal of Electronics and Communications*, Vol. 132, 153612, 2021.

[18] Esmail, B. A. F. and S. Koziel, "Design and optimization of metamaterial-based dual-band 28/38 GHz 5G MIMO antenna with modified ground for isolation and bandwidth improvement," *IEEE Antennas and Wireless Propagation Letters*, Vol. 22, No. 5, 1069–1073, May 2023.

[19] Singh, A. K. and S. Pal, "Compact self-isolated extremely low ECC folded-SIW-based slot MIMO antenna for 5G application," *IEEE Antennas and Wireless Propagation Letters*, Vol. 23, No. 1, 194–198, Jan. 2024.

[20] Cuneray, K., N. Akcam, T. Okan, and G. O. Arican, "28/38 GHz dual-band MIMO antenna with wideband and high gain properties for 5G applications," *AEU — International Journal of Electronics and Communications*, Vol. 162, 154553, Apr. 2023.

[21] Alieldin, A., Y. Huang, M. Stanley, S. D. Joseph, and D. Lei, "A 5G MIMO antenna for broadcast and traffic communication topologies based on pseudo inverse synthesis," *IEEE Access*, Vol. 6, No. 1, 65 935–65 944, 2018.